Int. J. Adv. Appl. Math. and Mech. 1(3) (2014) 121 - 134
ISSN: 2347-2529
Available online at www.ijaamm.com

IJAAMM

International Journal of Advances in **Applied Mathematics and Mechanics**

Transient thermophoretic particle deposition on MHD free convective and viscous dissipative flow along an inclined surface considering Dufour-Soret effects

Research Article

M. S. Alam[1]*

[1]*Department of Mathematics, Jagannath University, Dhaka-1100, Bangladesh*

Received 01 October 2013; accepted (in revised version) 11 March 2014

Abstract: In this paper thermophoretic particle deposition on an unsteady magnetodydrodynamic (MHD) free convective heat and mass transfer flow along an impulsively started infinite inclined porous plate under the influence of Dufour-Soret effects have been studied numerically. The transformed governing equations obtained by similarity transformations are solved by shooting method. Comparison with previously published work on special case of the problem were performed and found to be in very good agreement. The effects of various parameters on the dimensionless velocity, temperature, concentration distributions as well as wall themophoretic velocity are displayed graphically for a hydrogen-air mixture as the non-chemical reacting fluid pair. In addition, the predicted results for the local skin-friction coefficient, local Nusselt number and local Sherwood number are also tabulated. Wall thermophoretic velocity is increased with the increasing values of the thermophoretic parameter as well as suction parameter. The results also show that the presence of thermal diffusion and diffusion thermo intensify the shear stress but reduce the rate of heat and mass transfer.

MSC: 76M55 • 65L06

Keywords: Heat and mass transfer • Unsteady flow • Inclined plate • Dufour-Soret effects • Thermophoresis

1. Introduction

Deposition onto surfaces is a commonly observed phenomenon for small particles and recently this topic has gained importance for many engineering applications. The factors that influence particle depositions include convection, Brownian diffusion, turbulence, sedimentation, inertial effect, thermophoresis, electrophoresis and surface geometry, respectively. Among these factors, thermophoresis is important, when temperature gradient is very large and particle

* *Corresponding author. E-mail: dralamjnu@gmail.com*

Nomenclature

B_0	Magnetic induction
C	Concentration
Cf	Local skin-friction coefficient
C_p	Specific heat at constant pressure
D	Mass diffusivity
f	Dimensionless stream function
g	Acceleration due to gravity
Gr	Local Grashof number
Gm	Local modified Grashof number
M	Magnetic field parameter
Nu	Local Nusselt number
Pr	Prandtl number
Re_δ	Local Reynolds number
Sc	Schmidt number
Sh	Local Sherwood number
T	Temperature
Tr	Reference temperature
u, v	Velocity components in the x- and y-direction respectively
x, y	Axis in direction along and normal to the plate

Greek symbols

η	Pseudo-similarity variable
α	Angle of inclination to the vertical
β	Coefficient of thermal expansion
β^*	Coefficient of concentration expansion
σ	Electrical conductivity
ρ	Density of the fluid
ν	Kinematic viscosity
λ_g	Thermal conductivity of fluid
τ	Thermophoretic parameter
θ	Dimensionless temperature
ϕ	Dimensionless concentration

diameter lies between $0.1\mu m - 1.0\mu m$. With the increase of diameter, the inertia of the particles is growing, making the particles more easily to stray the flowing route of the flow, thus the inertia effect gradually replaces diffusion and thermophoretic effect to become the dominant deposition mechanism. Peterson et al. [1] studied two different model approaches for aerosol deposition on wafers and the particle concentration profile above a wafer surface. Sasse et al. [2] analyzed the concept of combining thermophoresis with natural convection flow for the design of a control device for capturing sidestream smoke particles. The approach involved numerical simulations of the competition among advection, diffusion, and thermophoresis within a channel between (a) parallel plates and (b) concentric tubes. Their numerical results showed that the temperature difference between the plates, with the cold wall fixed at ambient temperature, does not have a significant effect on the efficiency of particle removal. Tsai and Liang [3] adopted the numerical solutions for self-similar boundary layer flows to develop a rational correlation for evaluating the effect of thermophoresis on aerosol deposition from laminar flow system. In their model they have used the similarity method

to estimate the precipitation rates for dust, soot and mist from the aerosol flow. Sippola and Nazaroff [4] built the experimental ventilation ducts to measure the particle deposition in both fully developed and developing turbulent flow. Walsh et al. [5] investigated the thermophoretic deposition of aerosol particles in mixed convection, laminar tube flow with a cooled wall. Rahman and Postelnicu [6] studied effects of thermophoresis on the forced convective laminar flow of a viscous incompressible fluid over a rotating disk. Rahman et al. [7, 8] studied the thermophoresis particle deposition on unsteady two-dimensional forced convective heat and mass transfer flow along a wedge with variable fluid properties and variable Prandtl number. Very recently, Alam and Rahman [9] investigated thermophoretic particle deposition on unsteady hydromagnetic radiative heat and mass transfer flow along an infinite inclined permeable surface with viscous dissipation and Joule heating.

However, in the above studies, both the Dufour and Soret effects were neglected from the energy and concentration equations respectively, on the basis that they are of a smaller order of magnitude than the effects described by Fourier's and Fick's laws. There are, however, exceptions. The Soret effect, for instance, has been utilized for isotope separation and in mixture between gases and with very light molecular weight (H_2, He) and of medium molecular weight (H_2, air) the Dufour effect was found to be of considerable magnitude such that it cannot be neglected [10]. Kafoussias and Williams [11] included the Dufour and Soret effects on mixed free-forced convective and mass transfer flow where viscosity varies inversely proportional to the temperature. Anghel et al. [12] investigated the Dufour and Soret effects on free convection boundary layer over a vertical surface embedded in a porous medium. Postelnicu [13] studied the influence of a magnetic field on heat and mass transfer by natural convection from vertical surfaces in porous media considering Soret and Dufour effects. Lakshmi and Sibanda [14] investigated Soret and Dufour effects on free convection along a vertical wavy surface in a fluid saturated Darcy porous medium.

Therefore, the objective of the present paper is to study the effect of thermophoresis on an unsteady MHD free convection and mass transfer flow past an infinite inclined porous flat plate under the influence of Dufour-Soret effects.

2. Mathematical modeling

Let us consider an unsteady MHD free convection and mass transfer flow of an electrically conducting incompressible viscous fluid past an infinite inclined porous flat plate with an acute angleα to the vertical. The flow is assumed to be in the x-direction, which is taken along the inclined plate and y-axis normal to it. A magnetic field of uniform strength B_0 is introduced normal to the direction of the flow. Initially ($t = 0$) the plate and the fluid are at rest. But for time $t > 0$, the plate starts moving impulsively in its own plane with a velocity U_0, its temperature is raised to T_w which is higher than the ambient temperature T_∞. The species concentration at the surface is maintained uniform at C_w and that of the ambient fluid is assumed to be C_∞. Fluid suction is imposed at the plate surface. In addition, the effect of thermophoresis is taken into account as it helps in understanding mass deposition on surface. We further assume that (i) the magnetic Reynolds number is assumed to be small so that the induced magnetic field is negligible in comparison to the applied magnetic

field, (ii) due to the boundary layer behaviour the temperature gradient in the y direction is much larger than that in the x direction and hence only the thermophoretic velocity component which is normal to the surface is of importance, (iii) the fluid has constant kinematic viscosity and thermal diffusivity, and that the Boussinesq approximation may be adopted for unsteady laminar flow. Since the plate is of infinite extended all derivatives with respect to x are supposed to be zero and hence under the usual boundary-layer approximation, the governing equation for this problem can be written as follows:

Continuity equation,

$$\frac{\partial v}{\partial y} = 0 \tag{1}$$

Momentum equation,

$$\frac{\partial u}{\partial t} + v\frac{\partial u}{\partial y} = \upsilon\frac{\partial^2 u}{\partial y^2} + g\beta(T - T_\infty)\cos\alpha + g\beta^*(C - C_\infty)\cos\alpha - \frac{\sigma B_0^2}{\rho}u \tag{2}$$

Energy equation,

$$\frac{\partial T}{\partial t} + v\frac{\partial T}{\partial y} = \frac{\lambda_g}{\rho c_p}\frac{\partial^2 T}{\partial y^2} + \frac{D_m k_T}{c_s c_p}\frac{\partial^2 C}{\partial y^2} + \frac{\mu}{\rho c_p}\left(\frac{\partial u}{\partial y}\right)^2 \tag{3}$$

Diffusion equation,

$$\frac{\partial C}{\partial t} + v\frac{\partial C}{\partial y} = D\frac{\partial^2 C}{\partial y^2} + \frac{D_m k_T}{T_m}\frac{\partial^2 T}{\partial y^2} - \frac{\partial}{\partial y}[V_T(C - C_\infty)] \tag{4}$$

The initial and boundary conditions for the above problem are:

$$u = v = 0, \quad T = T_\infty, \quad C = C_\infty \quad \text{for} \quad t \le 0, \quad \text{for all} \quad y$$

$$\left.\begin{aligned} &u = U_0, \quad v = v(t), \quad T = T_w, \quad C = C_w \quad \text{for} \quad t > 0 \quad \text{at} \quad y = 0 \qquad (5a)\\ &u = 0, \quad v = 0, \quad T = T_\infty, \quad C = C_\infty \quad \text{for} \quad t > 0 \quad \text{as} \quad y \to \infty \qquad (5b) \end{aligned}\right\} \tag{5}$$

where $v(t)$ is the time dependent suction velocity at the porous plate. In equation (4), the thermophoretic velocity V_T can be written as,

$$V_T = -k\upsilon\frac{\nabla T}{T_r} = -\frac{k\upsilon}{T_r}\frac{\partial T}{\partial y} \tag{6}$$

where k is the thermophoretic coefficient and T_r is some reference temperature. Now in order to obtain a local similarity solution in time of the problem under consideration, we introduce a time dependent length scale δ as

$$\delta = \delta(t) \tag{7}$$

In terms of this length scale, a convenient solution of the equation (1) is considered to be in the following form,

$$v = v(t) = -v_0\frac{\upsilon}{\delta} \tag{8}$$

where v_0 is the suction parameter.

We now introduce the following dimensionless variables:

$$\left.\begin{aligned} &\eta = \tfrac{y}{\delta}, u = U_0 f(\eta), \\ &\theta(\eta) = \tfrac{T-T_\infty}{T_w-T_\infty}, \\ &\varphi(\eta) = \tfrac{C-C_\infty}{C_w-C_\infty}. \end{aligned}\right\} \tag{9}$$

Then introducing the relations (6)-(9) into the equations (2), (3) and (4) respectively, we then obtain the following ordinary differential equations:

$$f'' + (2\eta + v_0) f' + Gr\,\theta\cos\alpha + Gm\,\varphi\cos\alpha - Mf = 0 \tag{10}$$

$$\theta'' + \Pr(2\eta + v_0)\theta' + \Pr Df\varphi'' + \Pr Ec(f')^2 = 0 \tag{11}$$

$$\varphi'' + Sc(2\eta + v_0)\varphi' + \tau Sc(\varphi\theta'' + \varphi'\theta') + ScSo\theta'' = 0 \tag{12}$$

where $\Pr = \frac{\rho c_p \upsilon}{\lambda_g}$ is the Prandtl number, $Sc = \frac{\upsilon}{D}$ is the Schmidt number, $M = \frac{\sigma B_0^2 \delta^2}{\upsilon\rho}$ is the local Magnetic field parameter, $Gr = \frac{g\beta(T_w-T_\infty)\delta^2}{\upsilon U_0}$ is the local Grashof number, $Gm = \frac{g\beta^*(C_w-C_\infty)\delta^2}{\upsilon U_0}$ is the modified Grashof number, $So = \frac{D_m k_T (T_w-T_\infty)}{T_m \upsilon (C_w-C_\infty)}$ is the Soret number, $Df = \frac{D_m k_T (C_w-C_\infty)}{c_s c_p \upsilon (T_w-T_\infty)}$ is the Dufour number, $Ec = \frac{U_0^2}{c_p(T_w-T_\infty)}$ is the Eckert number and $\tau = \frac{k(T_w-T_\infty)}{T_r}$ is the thermophoretic parameter.

The corresponding boundary conditions for $t > 0$ are obtained as,

$$\left.\begin{aligned} &f = 1, \quad \theta = 1, \quad \varphi = 1 \quad \text{at} \quad \eta = 0 \qquad (13a) \\ &f = 0, \quad \theta = 0, \quad \varphi = 0 \quad \text{as} \quad \eta \to \infty \qquad (13b) \end{aligned}\right\} \tag{13}$$

The system of equations (10)-(12) under the boundary conditions (13) have been solved numerically by applying Nachtsheim-Swigert [15] shooting iteration technique together with sixth order Runge-Kutta integration scheme.

3. Local skin-friction coefficient, local Nusselt number and Sherwood number

Now it is important to calculate the physical quantities of the primary interest, which are the local wall shear stress, local surface heat flux and the local surface mass flux respectively from the following definitions:

$$\tau_w = \mu\left(\frac{\partial u}{\partial y}\right)_{y=0} \tag{14}$$

$$q_w = -\lambda\left(\frac{\partial T}{\partial y}\right)_{y=0} \tag{15}$$

$$M_w = -D\left(\frac{\partial C}{\partial y}\right)_{y=0} \tag{16}$$

Using equation (9), (14)-(16) can be written as

$$\tau_w = \mu U_0 \frac{1}{\delta} f'(0) \tag{17}$$

$$q_w = -\lambda_g (T_w - T_\infty) \frac{1}{\delta} \theta'(0) \tag{18}$$

$$M_w = -D(C_w - C_\infty) \frac{1}{\delta} \varphi'(0) \tag{19}$$

Hence the dimensionless local skin-friction coefficient, local Nusselt number and local Sherwood number for accelerated plate are given by

$$Cf = \frac{2\tau_w}{\rho U_0^2} = 2(\mathrm{Re}_\delta)^{-1} f'(0) \tag{20}$$

$$Nu = \frac{q_w \delta}{\lambda_g (T_w - T_\infty)} = -\theta'(0) \tag{21}$$

$$Sh = \frac{M_w \delta}{D(C_w - C_\infty)} = -\varphi'(0) \tag{22}$$

where $\mathrm{Re}_\delta = \frac{U_0 \delta}{\upsilon}$ is the local Reynolds number.

Of more technical interest for the present problem is the dimensionless wall thermophoretic velocity V_{TW}, which is given by

$$V_{TW} = \left(\frac{V_T \delta}{\upsilon} \right)_{y=0} = -\tau\, \theta(0) \tag{23}$$

4. Numerical solution

The system of nonlinear ordinary differential equations (10)-(12) together with the boundary conditions (13) are locally similar and are solved numerically by applying Nachtsheim-Swigert [15] shooting iteration technique along with sixth order Runge-Kutta integration scheme. For detailed discussion of the method see [16]. In equation (13) there are three asymptotic boundary conditions and hence three unknown surface conditions $f'(0)$, $\theta(0)$ and $\varphi(0)$. Thus adopting this numerical technique, a computer program was set up for the solutions of the governing non-linear partial differential equations of our problem where the integration technique was adopted as a sixth-order Runge-Kutta method of integration. Various groups of the parameters υ_0, Pr, Sc, Gr, Gm, α, τ, Ec, Df and So are considered in different phases. In all the computations the step size $\Delta\eta = 0.001$ was selected that satisfied a convergence criterion of 10ïĂ⬡6 in almost all of different phases mentioned above. The value of η_∞ was found to each iteration loop by the statement $\eta_\infty = \eta_\infty + \Delta\eta$. The maximum value of η_∞, to each group of parameters, has been obtained when the value of the unknown boundary conditions at $\eta = 0$ not change to successful loop with error less than 10^{-6}.

Table 1. Comparison of local skin-friction coefficient Cf local Nusselt number Nu and local Sherwood number Sh with [17] when $\alpha = Ec = \tau = 0$

So	Df	[17] Cf	Present Cf	[17] Nu	Present Nu	[17] Sh	Present Sh
2.0	0.03	7.205083	7.187874	1.934014	1.888343	0.087042	0.064950
0.4	0.15	5.775135	5.796955	1.517723	1.495787	0.495844	0.528549
0.1	0.60	5.581900	5.647452	1.364413	1.308114	0.575167	0.585167

Table 2. Effects of α and M on local skin-friction coefficient Cf, local Nusselt number Nu and local Sherwood number Sh for $Gr = 2, Gm = 10, Pr = 0.71, Sc = 0.22, \tau = 1, So = 0.2, Df = 0.30, Ec = 0.02$ and $\upsilon_0 = 0.50$

α	M	Cf	Nu	Sh
0°	0.0	5.5731844	1.1033246	0.7594292
0°	1.0	4.2347270	1.1033242	0.7594278
0°	2.0	3.2602316	1.1033237	0.7594260
30°	0.0	4.6303700	1.1033226	0.7594217
30°	1.0	3.4272046	1.1033222	0.7594204
30°	2.0	2.5457452	1.1033218	0.7594187
60°	0.0	2.0544172	1.1033162	0.7593978
60°	1.0	1.2209284	1.1033160	0.7593971
60°	2.0	0.5936759	1.1033157	0.7593961

5. Program validation and comparison with previous research

In order to check on the accuracy of the numerical technique employed for the solution of the problem considered in the present study, it was validated by performing simulation for local similarity solutions for unsteady MHD free convection and mass transfer flow past an impulsively started vertical porous plate with Dufour and Soret effects which are repoted by Alam et al. [17]. Table 1 shows the predicted values for local skin-friction coefficient, local Nusselt number and local Sherwood number for the present solution when $\alpha = \tau = 0$, and the results published by Alam et al [17]. Table 1 shows a very good agreement between the results and this lends credence to the present numerical code.

Table 3. Effects of τ, so and Df on local skin-friction coefficient Cf, local Nusselt number Nu and local Sherwood number Sh for $Gr = 2, Gm = 10, Pr = 0.71, Sc = 0.22, M = 0.50, \upsilon_0 = 0.50, Ec = 0.02$ and $\alpha = 30°$

τ	So	Df	Cf	Nu	Sh
0	0.0	0.000	2.7411273	1.1877866	0.6016154
2	0.0	0.000	2.1491859	1.1877817	1.0262100
4	0.0	0.000	1.6635905	1.1877780	1.4732441
0	0.2	0.300	2.8395935	1.1375576	0.5661670
2	0.2	0.300	2.2853644	1.0700317	0.9446537
4	0.2	0.300	1.8475460	1.0068258	1.2903904
0	0.8	0.075	3.0616637	1.1798726	0.4528795
2	0.8	0.075	2.4524486	1.1615250	08641766
4	0.8	0.075	1.9562444	1.1421985	1.2820864

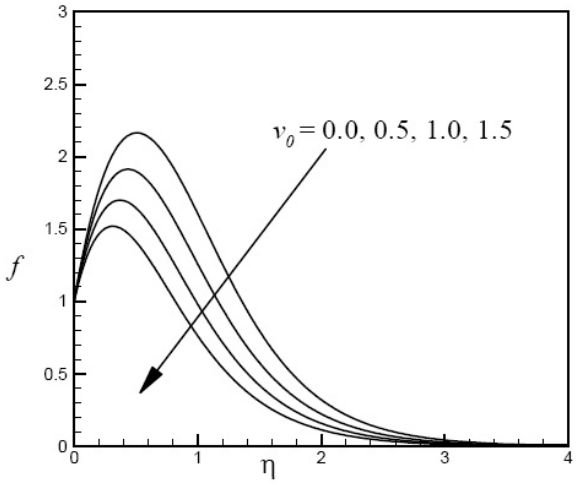

(a)

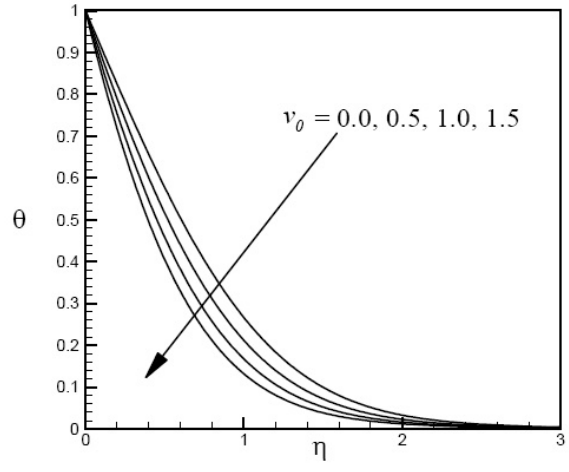

(b)

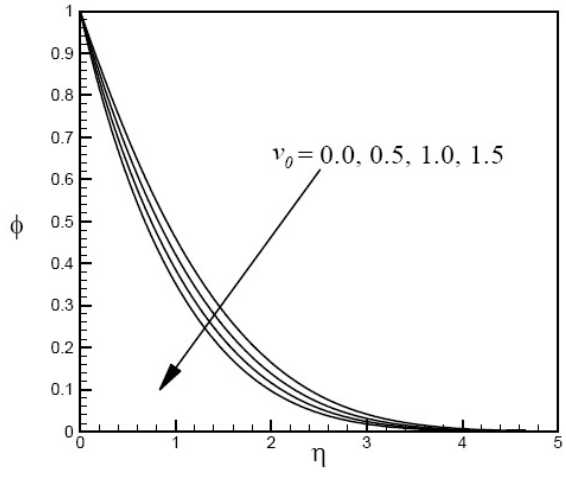

(c)

Figure 1. Dimensionless (a) velocity, (b) temperature and (c) concentration profiles for different values of v_0 and for $Gr = 2, Gm = 10, Pr = 0.71, Sc = 0.22, M = 0.50, Df = 0.30, S_l = 0.2, \tau = 1.0$ and $\alpha = 30°$

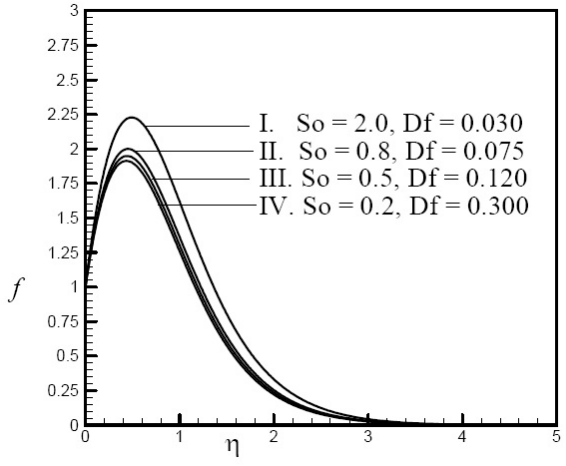

(a)

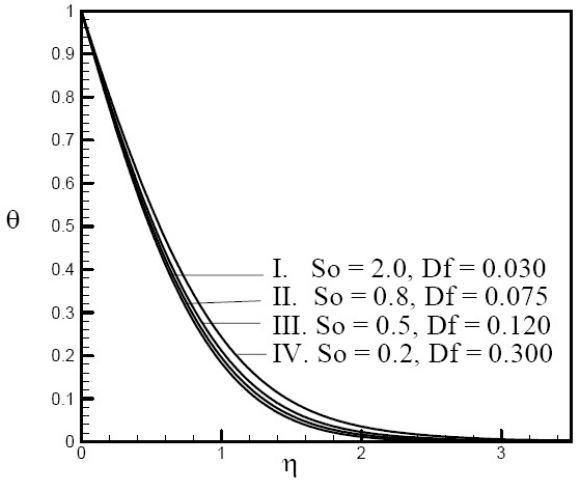

(b)

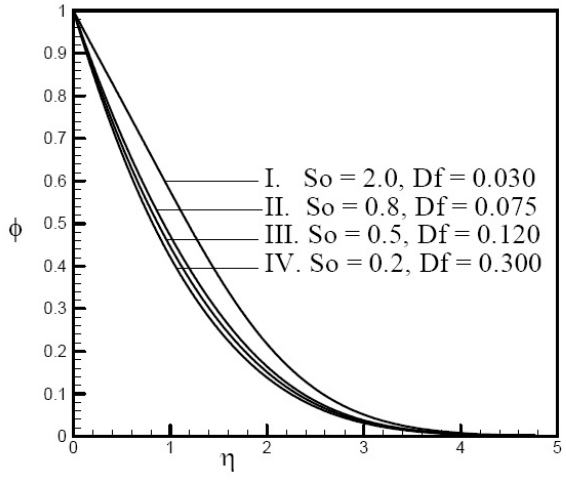

(c)

Figure 2. Dimensionless (a) velocity, (b) temperature and (c) concentration profiles for different values of Df and S_0 and for $Gr = 2, Gm = 10, Pr = 0.71, Sc = 0.22, v0 = 0.50, M = 0.50, = 1.0$ and $\alpha = 30°$

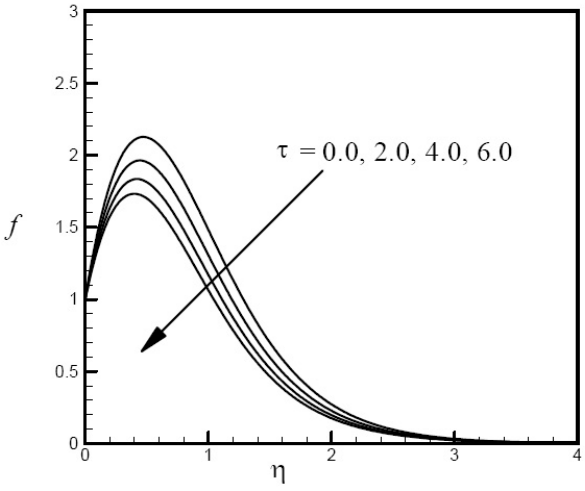

(a)

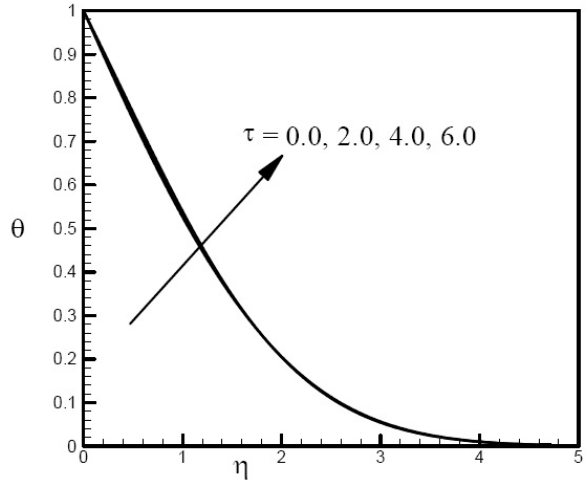

(b)

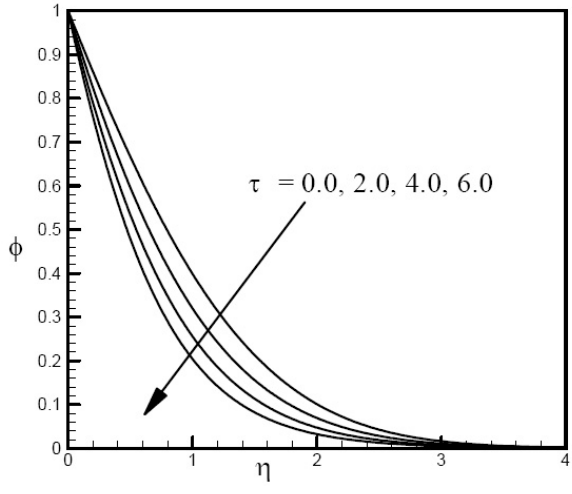

(c)

Figure 3. Dimensionless (a) velocity, (b) temperature and (c) concentration profiles for different values of τ and for $Gr = 2, Gm = 10, Pr = 0.71, Sc = 0.22, v0 = 0.50, M = 0.50, Df = 0.30, S_0 = 0.2$ and $\alpha = 30°$

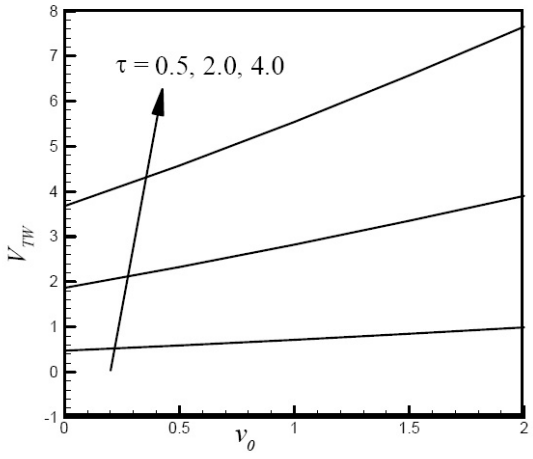

Figure 4. Effects of v_0 and τ on dimensionless wall thermophoretic velocity

6. Numerical results and discussion

The results of the numerical computations are displayed in Figs.1-4 respectively for dimensionless velocity, temperature, concentration fields and wall thermophoretic velocity for $Pr = 0.71, Gr = 2, Gm = 10, Sc = 0.22, Ec = 0.02$ and for different values of v_0, S_0, Df and τ. The values of $Pr = 0.71$ corresponds physically to the air, while the value $Sc = 0.22$ is chosen to represent hydrogen at appx. $25^{\circ}C$ and 1 atm.

The effects of suction parameter in the velocity field are shown in Fig. 1(a). It is found from this figure that the velocity profiles decrease monotonically with the increase of suction parameter indicating the usual fact that suction stabilizes the boundary layer growth. By sucking the slowed boundary layer, material into the inside of the body through narrow slits on the wall, boundary layer separation can be prevented. The free convection effect is also apparent in this figure. For fixed suction velocity (v_0), fluid velocity is found to increase and reaches a maximum value in a region close to the surface of the inclined plate, then gradually decreases to zero. The effect of suction parameter on the temperature and concentration field is displayed in Figs. 1(b) and 1(c) respectively and we see that both the temperature and concentration decreases with the increase of suction parameter. Sucking decelerated fluid particles through the porous wall reduce the growth of the hydrodynamic, thermal and concentration boundary layers.

The effects of Soret and Dufour numbers on the velocity field are shown in Fig. 2(a). We observe that quantitatively when $\eta = 1.0$ and S_o decreases from 2 to 0.8 (or Df increases from 0.03 to 0.075) there is 18.76% decrease in the velocity value, whereas the corresponding decrease is 3.48%, when S_o decreases from 0.5 to 0.2.

The effects of Soret and Dufour numbers on the temperature field are shown in Fig. 2(b). We observe that quantitatively $\eta = 1.0$ and S_o decreases from 2 to 0.8 (or Df increases from 0.03 to 0.075) there is 2.59 % increase in the temperature value, whereas the corresponding increase is 9.87 %, when S_o decreases from 0.5 to 0.2.

The effects of Soret and Dufour numbers on the concentration field are shown in Fig. 2(c). We observe that quantitatively

$\eta = 1.0$ and S_o decreases from 2 to 0.8 (or Df increases from 0.03 to 0.075) there is 22.17 % increase in the concentration value, whereas the corresponding increase is 5.31 %, when S_o decreases from 0.5 to 0.2.

The effects of thermophoretic parameter τ on the velocity, temperature as well as concentration distributions are displayed in Figs. 3(a)-3(c) respectively. It is observed from these figures that an increase in the thermophoretic parameter τ leads to decrease in the velocity across the boundary layer. This is accompanied by a decrease in the concentration and a slight increase in the fluid temperature. This means that the effect of increasing τ is limited to increasing the wall slope of the convection profile without any significant effect on the concentration boundary layer.

Fig. 4 represents the dimensionless wall thermophoretic velocity for different values of suction parameter v_0 and thermophoretic parameter τ. It is seen clearly from this figures that the wall thermophoretic velocity is increased with the increasing values of the thermophoretic parameter as well as suction parameter.

From Table 2 we see that all rates of shear stress, heat transfer and mass transfer decrease as the strength of the applied magnetic field intensifies. Thus, applied magnetic field controls the growth of the hydrodynamic, thermal and concentration boundary layer thicknesses. The effects of the angle of inclination on the skin friction coefficient, Nusselt number and Sherwood number are evident from Table 2. It is observed that skin friction coefficient and Sherwood number decrease whereas Nusselt number increases with the increase of the angle of inclination.

The effects of the thermophoretic parameter and Dufour-Soret number on rates of shear stress, heat transfer and mass transfer are tabulated in Table 3. It is found that rates of shear stress and rate of heat transfer decrease whereas the rate of mass transfer increases with the increase of the thermophoretic parameter. Table 3 further reveals that rate of shear stress and Nusselt number increase whereas rate of mass transfer decreases with the combined effect of the Soret (increasing value) and Dufour (decreasing value) numbers. It is also noticeable that the presence of thermal diffusion and diffusion thermo intensifies the skin friction coefficient but reduce the Nusselt and Sherwood numbers.

7. Conclusions

In this paper thermophoretic particle deposition on an unsteady magnetodydrodynamic (MHD) free convective heat and mass transfer flow along an impulsively started infinite inclined porous plate under the influence of Dufour-Soret effects have been studied numerically. The governing nonlinear partial differential equations are transformed into a set of coupled ordinary differential equations by using similarity transformation, which are then solved numerically by applying shooting method with sixth-order Runge-Kutta integration scheme. The present code is verified compared with existing data available in the literature and very good agreement is obtained. The effects of the pertinent parameters on the nondimensional velocity, temperature, concentration distributions as well as wall thermophoretic velocity are displayed graphically for a hydrogen-air mixture as a non-chemical reacting fluid pair. In addition, the local skin-friction coefficient, the local Nusselt number and the local Sherwood number are also tabulated to show physical aspects of the

solutions. From the present investigation the following major conclusions can be made:

- Suction stabilizes the boundary layer growth.
- Applied magnetic field controls the growth of the hydrodynamic, thermal as well as concentration boundary layer thicknesses.
- Wall thermophoretic velocity is increased with the increasing values of the thermophoretic parameter as well as suction parameter.
- The presence of thermal diffusion and diffusion thermo intensify the shear stress but reduce the rate of heat and mass transfer.

References

[1] T. W. Peterson, , F. Stratmann, H. Fissan, Particle deposition a wafers: A comparison between two modeling approaches. J. Aerosol Sci. 20(6) (1989) 483-493.

[2] A. G. B. M. Sasse,, W. W. Nazaroff, A. J. Gadgil, Particle filter based on thermophoretic deposition from natural convection. Aerosol Sci. and Tech. 20 (1994) 227-238.

[3] R. Tsai, L. J. Liang, Correlation for thermophoretic deposition of aerosol particles onto cold plates. J. Aerosol Sci. 32 (2001) 473-487.

[4] M. R. Sippola, W. W. Nazaroff, Experiments measuring particle deposition from fully developed turbulent flow in ventilation ducts. Aerosol Sci. and Tech. 38 (2004) 914-925.

[5] J. K. Walsh, A. W. Weimer, C. M. Hrenya, An experimental study of thermophoretic deposition of aerosol particles in laminar tube flow with mixed convection. Aerosol Sci. and Tech. 40 (2006) 178-188.

[6] M. M. Rahman, A. Postelnicu, Effects of thermophoresis on the forced convective laminar flow of a viscous incompressible fluid over a rotating disk. Mech. Res. Commun. 37 (2010) 598-603.

[7] M. M. Rahman, M. S. Alam, M. K. Chowdhury, Effects of variable thermal conductivity and variable Prandtl number on unsteady forced convective flow along a permeable wedge with suction/injection in the presence of thermophoresis. Int. J. Energy and Technology 4(4) (2012) 1-10.

[8] M. M. Rahman,, M. S. Alam, M. K. Chowdhury, Thermophoresis particle deposition on unsteady two-dimensional forced convective heat and mass transfer flow along a wedge with variable viscosity and variable Prandtl number. Int. Communications in Heat and Mass Transfer 39 (2012) 541-550.

[9] M. S. Alam, M. M. Rahman, Thermophoretic particle deposition on unsteady hydromagnetic radiative heat and mass transfer flow along an infinite inclined permeable surface with viscous dissipation and Joule heating. Engng. E-Transactions, 7(2) (2012) 116-126.

[10] E. R. G. Eckert,, R. M. Drake, Analysis of Heat and Mass Transfer, McGraw-Hill, New York, 1972.

[11] N. G. Kafoussias, E. W. Williams, Thermal-diffusion and diffusion-thermo effects on mixed free-forced convective and mass transfer boundary layer flow with temperature dependent viscosity, Int. J. Engng. Sci. 13 (1995) 1369-1384.

[12] M. Anghel, H. S. Takhar, I. Pop, Dufour and Soret effects on free-convection boundary layer over a vertical surface embedded in a porous medium. Studia Universitatis Babes-Bolyai, Mathematica XLV (2000) 11-21.

[13] A. Postelnicu, Influence of a magnetic field on heat and mass transfer by natural convection from vertical surfaces in porous media considering Soret and Dufour effects. Int. J. Heat Mass Transfer 47 (2004) 1467-1472.

[14] N. P. A. Lakshmi, P. Sibanda, Soret and Dufour effects on free convection along a vertical wavy surface in a fluid saturated Darcy porous medium. Int. J. Heat Mass Transfer 53 (2010) 3030-3034.

[15] P. R. Nachtsheim, P. Swigert, Satisfaction of the asymptotic boundary conditions in numerical solution of the system of nonlinear equations of boundary layer type. NASA TND-3004, 1965.

[16] M. S. Alam, M. M. Rahman, M. A. Samad, Numerical study of the combined free-forced convection and mass transfer flow past a vertical porous plate in a porous medium with heat generation and thermal diffusion. Non-linear Analysis: Modelling and Control 11 (2006) 331-343.

[17] M. S. Alam, M. M. Rahman, M. A. Maleque, Local similarity solutions for unsteady MHD free convection and mass transfer flow past an impulsively started vertical porous plate with Dufour and Soret effects. Thammasat Int. J. Sci. and Tech. 10(3) (2005) 1-8.